

Pure electron plasmas in asymmetric traps*

R. Chu and J. S. Wurtele

Department of Physics and Plasma Fusion Center, Massachusetts Institute of Technology, Cambridge, Massachusetts 02139

J. Notte, A. J. Peurrung, and J. Fajans†

Department of Physics, University of California at Berkeley, Berkeley, California 94720

(Received 1 December 1992; accepted 28 January 1993)

Pure electron plasmas are routinely confined within cylindrically symmetric Penning traps. In this paper the static and dynamic properties of plasmas confined in traps with applied electric field asymmetries are investigated. Simple analytical theories are derived and used to predict the shapes of the stable noncircular plasma equilibria observed in experiments. Both analytical and experimental results agree with those of a vortex-in-cell simulation. For an $\ell=1$ diocotron mode in a cylindrically symmetric trap, the plasma rotates as a rigid column in a circular orbit. In contrast, plasmas in systems with electric field asymmetries are shown to have an analog to the $\ell=1$ mode in which the shape of the plasma changes as it rotates in a noncircular orbit. These bulk plasma features are studied with a Hamiltonian model. It is seen that, for a small plasma, the area enclosed by the orbit of the center of charge is an invariant when electric field perturbations are applied adiabatically. This invariant has been observed experimentally. The breaking of the invariant is also studied. The dynamic Hamiltonian model is also used to predict the shape and frequency of the large amplitude $\ell=1$ and $\ell=2$ diocotron modes in symmetric traps.

I. INTRODUCTION

The equilibrium, stability, and dynamics of pure electron plasmas have been studied extensively.^{1,2} Traditionally, these plasmas are confined in Penning-like traps with cylindrical equipotential walls. Since these traps are azimuthally symmetric, the canonical angular momentum of the confined plasmas is conserved. This limits the radial expansion of the plasmas and has been thought to be responsible for the excellent confinement properties of these traps.³ However, the azimuthal symmetry can be broken by applying asymmetric electrostatic perturbations on the cylindrical trap wall. Experimental results⁴ prove that these asymmetries degrade, but do not destroy, the trap confinement properties. Because angular momentum need not be conserved, a new outlook is required to understand these plasmas.

In this paper we study the static and dynamic properties of pure electron plasmas confined in such asymmetric traps. The plasma drift dynamics studied here is assumed to occur on a slow time scale (T_d) compared to the cyclotron orbit time scale (T_c). Furthermore, the plasma is taken to be short and hot. Consequently the axial bounce period (T_b) along the magnetic field is also fast compared to the drifts. Thus, we use the guiding center approximation, and the electric field experienced by the electrons can be approximated by the bounce-averaged electric field. The observable dynamics reduce to two-dimensional, bounce-

averaged $\mathbf{E} \times \mathbf{B}$ drifts. For typical experimental parameters, $T_d \sim 10^{-6}$ sec, $T_b \sim 10^{-7}$ sec, and $T_c \sim 10^{-10}$ sec.

The continuity equation along with the $\mathbf{E} \times \mathbf{B}$ drifts and the Poisson equation provide a closed description of our system. Since the two-dimensional drift-Poisson equations governing the magnetized electron column dynamics are isomorphic to the Euler equations governing a constant density inviscid fluid,^{5,6} with the density and the electrostatic potential corresponding to the vorticity and the streamfunction in fluid dynamics, respectively, direct fluid analogies of the results presented in this paper can be drawn.

In Sec. II, we describe the response of a plasma, which is initially in equilibrium in an axisymmetric field, to a slowly applied azimuthal asymmetry. An analytical model is developed to give the approximate shapes of the asymmetric equilibria which are reached after the perturbations have reached their final values. These equilibria have also been observed in experiments.⁴ When the azimuthal perturbations are small, the asymmetric equilibria deviate only slightly from their unperturbed circular shapes, and we show explicitly that such equilibria are linearly stable. Furthermore, the shapes found with a particle simulation are compared to both the analytical and experimental results.⁴ In Sec. III, a Hamiltonian model for the plasma dynamics is developed and equations for the motion of the center of the plasma, its ellipticity, and its orientation are systematically derived. With a small plasma, the area enclosed by the $\ell=1$ diocotron orbit is shown to be an adiabatic invariant when azimuthal perturbations are applied. This invariant has been observed experimentally.⁷ We

*Paper 612, Bull. Am. Phys. Soc. 37, 1497 (1992).

†Invited speaker.

study both the existence and the breaking of this invariant. The Hamiltonian formalism developed here is useful in studying both symmetric and asymmetric systems. In Sec. IV, we use the elliptical plasma model to study the shape and frequency of the $\ell=1$ and $\ell=2$ diocotron modes, as functions of the displacement and plasma area, in symmetric traps.

II. STATIC EQUILIBRIA

A pure electron plasma confined within an azimuthally symmetric trap has a cylindrical equilibrium shape; asymmetric equilibrium shapes are obtained by slowly applying azimuthal asymmetries. Specifically, we have studied plasma asymmetries created by nonzero voltages applied to angular sectors of the confining cylindrical wall. Figure 1 shows an asymmetric plasma confined in such a trap. The asymmetry is ramped up over a time which is long compared to the plasma $\mathbf{E} \times \mathbf{B}$ rotation period so as not to excite any oscillatory motions. The plasma responds to these perturbations by slowly deforming into an asymmetric equilibrium shape which is stationary in the lab frame. Experimentally, such plasmas are stable and have relatively long lifetimes (tens of seconds).⁴

The two-dimensional $\mathbf{E} \times \mathbf{B}$ drift dynamics are governed by the velocity equation, $\mathbf{v} = -(c/B)\nabla\phi \times \hat{e}_z$, the Poisson equation, $\nabla^2\phi = 4\pi en$, and the continuity equation, $\partial n/\partial t + \mathbf{v} \cdot \nabla n = 0$. The theoretical model of these noncircular plasmas is based on the fact that the guiding centers drift along the equipotential contours. For a constant density plasma, the stationary shape requirement is satisfied if the plasma boundary lies on an equipotential contour. Hence, the condition for the plasma shape to be stationary is

$$\phi[r_p(\theta), \theta] = \phi_p[r_p(\theta), \theta] + \phi_a[r_p(\theta), \theta] = \text{const}, \quad (1)$$

where $r_p(\theta)$ specifies the boundary of the uniform density plasma, ϕ_p is the potential resulting from the charge of the plasma itself, and ϕ_a is the potential due to the (asymmetric) perturbations applied to the azimuthal sectors of the cylinder. The plasma potential, ϕ_p can be expressed in integral form as a convolution of the density with a Green's function for Gauss's law in cylindrical geometry. Since the nonaxisymmetric boundary conditions are included in ϕ_a , one must have $\phi_p = 0$ on the confining wall.

$$\phi_p(r, \theta) = -en \int_0^{2\pi} d\theta' \int_0^{r_p(\theta')} dr' r' \times \ln \left[\frac{R^4 + r^2 r'^2 - 2R^2 r r' \cos(\theta - \theta')}{R^2 [r^2 + r'^2 - 2r r' \cos(\theta - \theta')]} \right], \quad (2)$$

where R is the radius of the confining cylinder, and n is the density of the plasma.

Since the $\mathbf{E} \times \mathbf{B}$ flow is incompressible, the cross-section area of the asymmetric plasma will be the same as the cross-section area of the initial circular plasma. To reflect this conservation of area, the shape of the plasma is written as a Fourier series,

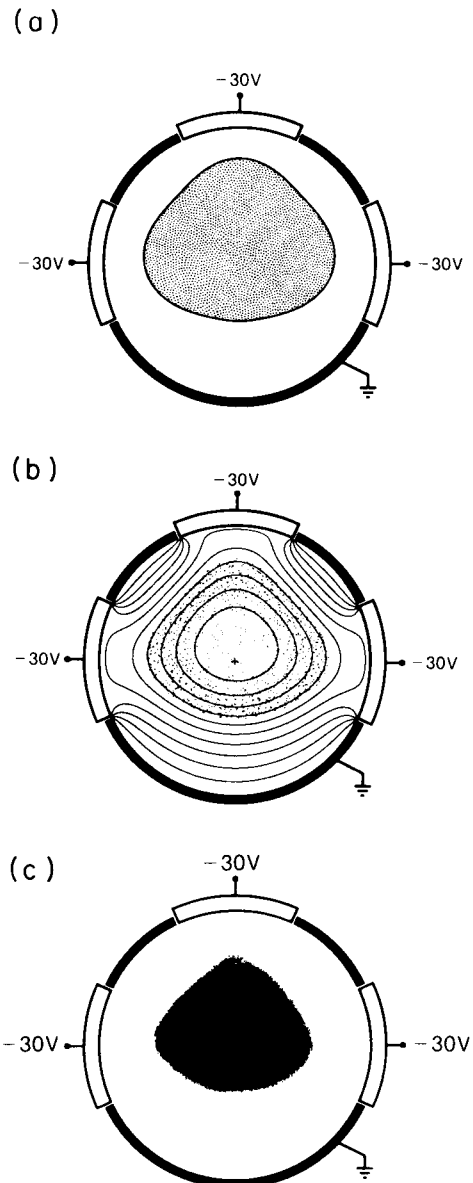


FIG. 1. (a) Plasma shape as determined by the analytical model. Density of the plasma, n , is $2.7 \times 10^7 \text{ cm}^{-3}$. (b) Plasma shape and equipotentials determined from the simulation. The separatrix lies between the closed and unclosed equipotential contours. (c) Experimentally observed plasma shape.

$$r_p^2(\theta) = r_0^2 + 2r_0 \sum_{l=1}^{\infty} [\delta r_l^c \cos(l\theta) + \delta r_l^s \sin(l\theta)], \quad (3)$$

where r_0 is the radius of the initial circular plasma. Expanding the above expression gives

$$\begin{aligned} r_p(\theta) &= r_0 + \delta r(\theta) \\ &= r_0 + \sum_{l=1}^{\infty} [\delta r_l^c \cos(l\theta) + \delta r_l^s \sin(l\theta)] + \mathcal{O}(\delta r_l^2). \end{aligned} \quad (4)$$

Substituting $r_p(\theta)$ in Eq. (4) into Eq. (2) and evaluating the integral by expanding the Green's function yields

$$\phi_p(r, \theta) = 2\pi en \begin{cases} r_0^2 \ln\left(\frac{r}{R}\right) + \sum_{l=1}^{\infty} \frac{1}{l} \left[\left(\frac{r}{R}\right)^l - \left(\frac{R}{r}\right)^l \right] \left(\frac{r_0}{R}\right)^l r_0 [\delta r_l^c \cos(l\theta) + \delta r_l^s \sin(l\theta)] + \mathcal{O}(\delta r_l^2) & \text{outside the plasma,} \\ \frac{r^2}{2} + r_0^2 \left[\ln\left(\frac{r_0}{R}\right) - \frac{1}{2} \right] + \sum_{l=1}^{\infty} \frac{1}{l} \left[\left(\frac{r_0}{R}\right)^l - \left(\frac{R}{r_0}\right)^l \right] \left(\frac{r}{R}\right)^l r_0 [\delta r_l^c \cos(l\theta) + \delta r_l^s \sin(l\theta)] + \mathcal{O}(\delta r_l^2) & \text{inside the plasma.} \end{cases} \quad (5)$$

It should be noted that truncating ϕ_p at order δr_l is equivalent to approximating it by the potential of the unperturbed circular plasma with the appropriate surface charge density, $\sigma(\theta) = n\delta r(\theta)$. The applied electrostatic potential, ϕ_a , can also be expressed as a Fourier series,

$$\phi_a(r, \theta) = A_0 + \sum_{l=1}^{\infty} \left(\frac{r}{R}\right)^l [A_l^c \cos(l\theta) + A_l^s \sin(l\theta)], \quad (6)$$

where the coefficients, $A_l^{c,s}$, are readily determined from the applied potentials. The total field, $\phi = \phi_p + \phi_a$, can now be expressed in terms of the applied boundary perturbation, $\phi_a(R, \theta)$, and the shape of the plasma column, δr_l .

The equilibrium condition [Eq. (1)] relates the perturbation in the plasma shape, δr_b , to the applied voltages on the wall, $\phi_a(R, \theta)$, for an asymmetric equilibrium. If the applied field perturbation is assumed to be small compared to the self-field of the plasma ($A_l \ll 2\pi en r_0^2$), then the deviation from a circular shape is also small ($\delta r_l \ll r_0$), and only the lowest order terms in A_l and δr_l in Eq. (1) need to be retained. The shape of the asymmetric plasma column in terms of the boundary perturbation is then

$$\delta r_l^{c,s} = -\frac{(r_0/R)^l}{2\pi en r_0 \{1 - [1 - (r_0/R)^{2l}]/l\}} A_l^{c,s}. \quad (7)$$

In addition to this simple analytic theory, a two-dimensional vortex-in-cell electrostatic code has also been used to examine these equilibria. A circular assembly of 4096 line charges is used to model an initial, circular plasma. The asymmetry is then applied by slowly changing the potential on the angular sectors of the confining wall. The simulation is time-advanced by first weighting the plasma to a uniform polar grid, then solving the Poisson equation, and finally, moving the line charges according to the $\mathbf{E} \times \mathbf{B}$ dynamics.

The success of the analytic theory [Fig. 1(a)] and the simulation [Fig. 1(b)] can be seen from the close agreement of these results with the corresponding experimental plasma⁴ [Fig. 1(c)]. A correction factor has been used to compare the infinite length results of Fig. 1(a) and Fig. 1(b) with the finite length experimental result. We assume that the electrons respond to the bounce-averaged fields of the finite length angular sectors. Bounce-averaging the electric field over the actual length of the plasma in the experiments indicates that the finite length angular sector is about 60% as effective as an infinite length sector. The potentials shown in Fig. 1(a) and Fig. 1(b) have been adjusted by this factor of 0.6.

The stability of energy conserving nonneutral plasmas has been investigated by O'Neil and Smith⁸ using varia-

tional techniques. In $\mathbf{E} \times \mathbf{B}$ guiding center drift dynamics, the energy of the system is purely electrostatic. The plasma equilibrium is locally stable to $\mathbf{E} \times \mathbf{B}$ dynamics if its energy is extremal when compared to the energy of all the nearby accessible states. The energy, \mathcal{E} , of any arbitrarily shaped plasma is given by

$$\mathcal{E} = -en \int d^2x \left(\frac{1}{2} \phi_p + \phi_a \right), \quad (8)$$

where the integration is performed over the plasma region. Substituting ϕ_p in Eq. (5) and ϕ_a in Eq. (6) into Eq. (8), and keeping terms up to second order in A_l and δr_b gives:

$$\begin{aligned} \mathcal{E} = & -\pi en r_0 \sum_{l=1}^{\infty} \left(\left(\frac{r_0}{R}\right)^l (\delta r_l^c A_l^c + \delta r_l^s A_l^s) \right. \\ & \left. + \pi en r_0 \left[1 - \frac{1}{l} \left[1 - \left(\frac{r_0}{R}\right)^{2l} \right] \right] [(\delta r_l^c)^2 + (\delta r_l^s)^2] \right). \end{aligned} \quad (9)$$

The terms which represent the interaction energy of the undistorted plasma with its self-field, its image, and the applied field are independent of δr_b , and have been omitted. When the plasma energy is at an extremum, the first derivatives of the plasma energy with respect to any change in the plasma shape must be zero:

$$\begin{aligned} 0 = \frac{d\mathcal{E}}{d\delta r_l^{c,s}} = & -\pi en r_0 \left(\left(\frac{r_0}{R}\right)^l A_l^{c,s} \right. \\ & \left. + 2\pi en r_0 \left[1 - \frac{1}{l} \left[1 - \left(\frac{r_0}{R}\right)^{2l} \right] \right] \delta r_l^{c,s} \right). \end{aligned} \quad (10)$$

Solving this equation yields the same expression for the shape of the plasma as a function of the boundary perturbation as was found earlier [Eq. (7)]. This solution is proved to be an energy maximum by establishing that the diagonal second derivatives are less than zero:

$$\frac{d^2\mathcal{E}}{d(\delta r_l^{c,s})^2} = -2(\pi en r_0)^2 \left[1 - \frac{1}{l} \left[1 - \left(\frac{r_0}{R}\right)^{2l} \right] \right] < 0, \quad (11)$$

and the off-diagonal second derivatives are exactly zero. Hence, the plasma deforms to the shape that maximizes the energy consistent with keeping its area invariant. This maximal energy principle also explains why the negatively charged plasma is attracted to negative imposed asymmetries and repelled from positive imposed asymmetries; such movements clearly maximize its energy. Other interesting properties of these asymmetric plasma equilibria are discussed in more detail in another paper.⁴

III. BULK PLASMA DYNAMICS

In the last section, we studied the centrally located asymmetric equilibria. In this section, we turn our attention to the bulk dynamics of the plasmas when they are displaced off-center. The mode which we study is the analog of the neutrally stable $\ell=1$ diocotron mode⁹ of a cylindrically symmetric system. When an electron plasma column is displaced from the center of the grounded conducting cylinder, the induced image charge on the cylindrical wall creates a radial electric field which causes the plasma column to $\mathbf{E} \times \mathbf{B}$ drift in the azimuthal direction. Consequently the plasma column orbits the center of the trap. This neutrally stable circular motion is called the $\ell=1$ diocotron mode, and we define A_ϕ to be the area enclosed by the orbit of the plasma's center of charge. The shape of the plasma column is invariant as it circles the trap axis; however, the plasma column assumes a near elliptical shape as the mode amplitude is increased.

When a bias is applied to a section of the cylindrical wall, the circular orbit is distorted, and the plasma shape changes continuously throughout the orbit. We find that A_ϕ is an adiabatic invariant of the system if the plasma is small. That is, a slowly applied perturbation will change the shape of the orbit without changing the area of the orbit. Further, we find that rapidly applied perturbations will change A_ϕ , in a manner similar to well-known examples of adiabatic invariant breaking. The adiabatic invariance of the orbital area has also been observed experimentally.⁷

We study this phenomenon using a guiding center Hamiltonian. The plasma is modeled as a collection of line charges, each with a given charge per unit length, q . When the magnetic field, \mathbf{B} , is constant, it can be shown that the Hamiltonian describing the $\mathbf{E} \times \mathbf{B}$ drift dynamics is just the electrostatic energy per unit length,

$$\begin{aligned}
 H(r_1, \theta_1, r_2, \theta_2, \dots, t) &= q \sum_i \phi_a(r_i, \theta_i, t) + q^2 \sum_i \ln \left(1 - \frac{r_i^2}{R^2} \right) \\
 &\quad - q^2 \sum_{i>j} \ln \left(\frac{r_i^2 + r_j^2 - 2r_i r_j \cos(\theta_i - \theta_j)}{R^2} \right) \\
 &\quad + q^2 \sum_{i>j} \ln \left(\frac{R^4 + r_i^2 r_j^2 - 2R^2 r_i r_j \cos(\theta_i - \theta_j)}{R^4} \right), \quad (12)
 \end{aligned}$$

where (r_i, θ_i) is the location of the i th guiding center. The momentum variable conjugate to θ_i is P_i , where $P_i = (qB/2c)r_i^2$. The first two terms on the right represent the interaction energy of each line charge with the applied potential, and with its own image. The third and fourth terms account for the interaction energy of each line charge with the other line charges and their images. Since we are interested in the dynamics of the center of charge, a canonical transformation can be performed to isolate the canonical pair θ_c and $P_c = (NqB/2c)r_c^2$, where (r_c, θ_c) is the location of the center of charge, from the other $N-1$ pairs which specify the shape and orientation of the plasma.

The dynamics described by the N -particle Hamiltonian is, in general, quite complicated. However, the analysis is greatly simplified if the plasma is assumed to be elliptical. The Hamiltonian in Eq. (12) can then be evaluated in the continuum limit, where $q\sum_i \rightarrow -en \int d^2x$, and $q^2\sum_{i>j} \rightarrow (e^2 n^2/2) \int d^2x' \int d^2x$, as a function of the dynamical variables r_c , θ_c , λ , and φ . Here $\lambda (> 1)$ is the aspect ratio of the elliptical plasma, and φ is the angle between its major axis and the x -axis. In evaluating the integrals for the interaction energy of the plasma with its image and the applied potential over the plasma region, the integrands are Taylor expanded about the plasma center. In the resulting series, $A_p/\pi R^2$ is treated as a small parameter, and only the lowest-order interaction terms are shown below. The quantity, A_p , is the area of the plasma, and is constant under $\mathbf{E} \times \mathbf{B}$ dynamics. The Hamiltonian can be broken into three parts, $H = H_s + H_c + H_\lambda$, where

$$H_s = -\frac{(enA_p)^2}{2} \ln \left(\frac{(1+\lambda)^2}{4\lambda} \right), \quad (13)$$

$$H_c = -enA_p \phi_a(r_c, \theta_c, t) + (enA_p)^2 \ln \left(1 - \frac{r_c^2}{R^2} \right), \quad (14)$$

$$\begin{aligned}
 H_\lambda &= \frac{enA_p^2}{8\pi} \left(\frac{1-\lambda^2}{\lambda} \right) \left(\frac{2enA_p r_c^2}{(R^2 - r_c^2)^2} \cos 2(\theta_c - \varphi) \right. \\
 &\quad + \cos 2(\theta_c - \varphi) \frac{\partial^2 \phi_a}{\partial r_c^2} - \frac{\sin 2(\theta_c - \varphi)}{r_c} \frac{\partial^2 \phi_a}{\partial r_c \partial \theta_c} \\
 &\quad \left. + \frac{\sin 2(\theta_c - \varphi)}{r_c^2} \frac{\partial \phi_a}{\partial \theta_c} \right) + \dots \quad (15)
 \end{aligned}$$

Here, H_s is the exact self-interaction energy of an elliptical plasma in free space, H_c is the interaction energy of a circular plasma or a line charge with the applied field and its own image, and H_λ is a series expansion of the interaction energy with the image and the applied field due to the deviation of the elliptical shape from a circle. When the plasma is circular, $\lambda=1$ and H_λ vanishes. In the series expansion of H_λ , higher-order terms can be kept to improve the accuracy of this model. This elliptical plasma model is similar to those used in fluid mechanics to study the interactions between two vortices.¹⁰⁻¹²

With Nq replaced by $-enA_p$, $P_c = -(BenA_p/2c)r_c^2$ is the momentum conjugate variable to θ_c . Furthermore,

$$P_\varphi = -\left(\frac{BenA_p}{2c} \right) \left(\frac{A_p}{4\pi} \right) \left(\frac{1+\lambda^2}{\lambda} \right)$$

is the variable conjugate to φ . The total canonical angular momentum per unit length, L , is

$$\begin{aligned}
 L &= -\frac{Ben}{2c} \int r^2 d^2x = -\frac{BenA_p}{2c} \left[r_c^2 + \left(\frac{A_p}{4\pi} \right) \left(\frac{1+\lambda^2}{\lambda} \right) \right] \\
 &= P_c + P_\varphi. \quad (16)
 \end{aligned}$$

When there is no applied field, i.e., when $\phi_a = 0$, the Hamiltonian reduces to a function of $\theta_c - \varphi$ due to the azimuthal symmetry. It can be seen easily that the canonical angular momentum in such a system is conserved in our

model ($\dot{L} = 0$). Since there are two pairs of canonical variables, the elliptical plasma model is a system with two degrees of freedom. In the asymmetric system, the angular momentum is no longer a constant, and hence the elliptical plasma model is, in general, not integrable when azimuthal symmetry is broken. However, if H_λ is ignored, the motion becomes integrable because the Hamiltonian consists of the sum of two separated and noninteracting pieces, H_s and H_c . The motion in the (λ, φ) phase space is determined by H_s alone, and the motion in the (r_c, θ_c) phase space, is

solely determined by H_c . Unfortunately, attempts to analyze the full model using classical perturbation theory, in which H_λ is treated as perturbation to the integrable system described by H_s and H_c , are nontrivial because the angle-action variables for H_c cannot be identified (due to the transcendental equations involved).

However, the equations of motion can be solved numerically. With H_λ approximated by the terms shown in Eq. (15), the full equations of motion of the elliptical plasma model are

$$\dot{r}_c = \frac{c}{B} \left[-\frac{1}{r_c} \frac{\partial \phi_a}{\partial \theta_c} + \frac{A_p}{8\pi} \left(\frac{1-\lambda^2}{\lambda} \right) \left(-\frac{4enA_p r_c}{(R^2-r_c^2)^2} \sin 2(\theta_c-\varphi) - \frac{2 \sin 2(\theta_c-\varphi)}{r_c} \frac{\partial^2 \phi_a}{\partial r_c^2} + \frac{\cos 2(\theta_c-\varphi)}{r_c} \frac{\partial^3 \phi_a}{\partial r_c^2 \partial \theta_c} - \frac{2 \cos 2(\theta_c-\varphi)}{r_c^2} \frac{\partial^2 \phi_a}{\partial r_c \partial \theta_c} - \frac{\sin 2(\theta_c-\varphi)}{r_c^2} \frac{\partial^3 \phi_a}{\partial r_c \partial \theta_c^2} + \frac{2 \cos 2(\theta_c-\varphi)}{r_c^3} \frac{\partial \phi_a}{\partial \theta_c} + \frac{\sin 2(\theta_c-\varphi)}{r_c^3} \frac{\partial^2 \phi_a}{\partial \theta_c^2} \right) \right], \quad (17)$$

$$\dot{\theta}_c = \frac{2cenA_p}{B(R^2-r_c^2)} \left[1 - \frac{A_p(R^2+r_c^2)}{4\pi(R^2-r_c^2)^2} \left(\frac{1-\lambda^2}{\lambda} \right) \cos 2(\theta_c-\varphi) \right] - \frac{c}{Br_c} \left[-\frac{\partial \phi_a}{\partial r_c} + \frac{A_p}{8\pi} \left(\frac{1-\lambda^2}{\lambda} \right) \left(\cos 2(\theta_c-\varphi) \frac{\partial^3 \phi_a}{\partial r_c^3} - \frac{\sin 2(\theta_c-\varphi)}{r_c} \frac{\partial^3 \phi_a}{\partial r_c^2 \partial \theta_c} + \frac{2 \sin 2(\theta_c-\varphi)}{r_c^2} \frac{\partial^2 \phi_a}{\partial r_c \partial \theta_c} - \frac{2 \sin 2(\theta_c-\varphi)}{r_c^3} \frac{\partial \phi_a}{\partial \theta_c} \right) \right], \quad (18)$$

$$\dot{\lambda} = -\frac{2c}{B\lambda} \left(\frac{2enA_p r_c^2}{(R^2-r_c^2)^2} \sin 2(\theta_c-\varphi) + \sin 2(\theta_c-\varphi) \frac{\partial^2 \phi_a}{\partial r_c^2} + \frac{\cos 2(\theta_c-\varphi)}{r_c} \frac{\partial^2 \phi_a}{\partial r_c \partial \theta_c} - \frac{\cos 2(\theta_c-\varphi)}{r_c^2} \frac{\partial \phi_a}{\partial \theta_c} \right), \quad (19)$$

$$\dot{\varphi} = \frac{c}{B} \left[4en\pi \frac{\lambda}{(1+\lambda)^2} - \frac{1+\lambda^2}{1-\lambda^2} \left(\frac{2enA_p r_c^2}{(R^2-r_c^2)^2} \cos 2(\theta_c-\varphi) + \cos 2(\theta_c-\varphi) \frac{\partial^2 \phi_a}{\partial r_c^2} - \frac{\sin 2(\theta_c-\varphi)}{r_c} \frac{\partial^2 \phi_a}{\partial r_c \partial \theta_c} + \frac{\sin 2(\theta_c-\varphi)}{r_c^2} \frac{\partial \phi_a}{\partial \theta_c} \right) \right]. \quad (20)$$

A simplification of the model is achieved by assuming that the shape of the plasma remains circular, i.e., $\lambda=1$. The orientation, φ , is then not defined, H_s is constant, and H_λ vanishes. The effective Hamiltonian of the system is just H_c , and the equations of motion reduce to

$$\dot{r}_c = -\frac{c}{Br_c} \frac{\partial \phi_a}{\partial \theta_c}, \quad (21)$$

$$\dot{\theta}_c = \frac{c}{B} \left(\frac{2enA_p}{R^2-r_c^2} + \frac{1}{r_c} \frac{\partial \phi_a}{\partial r_c} \right). \quad (22)$$

Since only one degree of freedom is left in the circular plasma model, the system is integrable. These simplified equations can also be found by modeling the plasma column as a line charge which carries the same charge per unit length, $-enA_p$. In other words, we take the limit $A_p \rightarrow 0$, while keeping the charge per unit length, $-enA_p$, constant. In this limit, $H_\lambda \rightarrow 0$, and the Hamiltonian separates into two noninteracting pieces, H_s and H_c . The motion in the (r_c, θ_c) phase space is then determined by H_c only, yielding Eqs. (21) and (22), as in the circular plasma model described earlier.

These two different simplifications yield the same equations of motion for (r_c, θ_c) because the image charge on the confining wall induced by a uniform density cylindrical plasma is exactly the same as that induced by a line charge. In addition, the image field and the applied field averaged over a constant density cylindrical plasma column is equal to that at the center of the column. Since the motion of the center of charge of an arbitrarily shaped plasma, in $\mathbf{E} \times \mathbf{B}$ dynamics, does not depend on its self-field (the self-field does not include the image field), the two sets of equations of motion should be identical.

The dynamics of the elliptical plasma model [Eqs. (17)–(20)] can be compared with the results of the simplified line charge model [Eqs. (21) and (22)]. In Fig. 2, the orbit of a line charge is compared with the orbits of two elliptical plasmas of different sizes but the same total charge (both with $\lambda=2$ initially). In this test, the bias applied to the angular sector is held constant. The center of charge motion shown in Fig. 2 was obtained by numerically integrating the two models. The orbit of the small elliptical plasma is nearly indistinguishable from the orbit of the line charge, although the shape of the elliptical plasma undergoes considerable fluctuations (λ varies be-

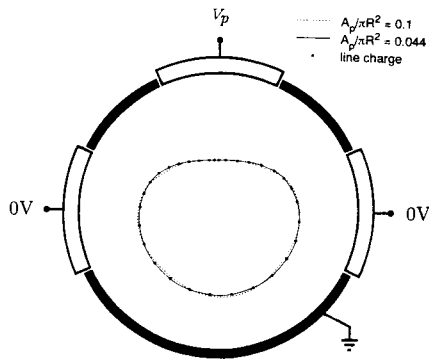


FIG. 2. Center of charge orbits of a line charge and two elliptical plasmas (carrying the same total charge) for $V_p/enA_p = 1.15$.

tween 2.0 and 2.5). The orbit of the larger plasma is only slightly different. Thus the energy change associated with a variation in the ellipticity or orientation of the plasma is small compared to the energy change associated with the motion of the center of charge, and we conclude that the simple line charge model (equivalent to the circular plasma model) is successful in predicting the center of charge orbits when the plasma is small. A similar decoupling of the elliptical variations from the center of charge motion has been observed for the case of two interacting vortices.¹³

Since the system described by the circular plasma model is one dimensional, the motion is always periodic in the phase space (P_θ, θ_c) (Ref. 14) when ϕ_a is time independent. Hence, the set of orbits is a nested set of nonintersecting loops, each with a unique orbital area and total electrostatic energy. A set of such orbits are shown in Fig. 3 when a constant bias, V_p , is put on an angular sector. When the externally applied perturbation is slowly varying, the area enclosed by the phase space orbit is an adiabatic invariant:¹⁴

$$\oint p dq = - \left(\frac{BenA_p}{c} \right) \oint \frac{r_c^2}{2} d\theta_c = - \left(\frac{BenA_p}{c} \right) A_\Phi. \quad (23)$$

Thus, the area enclosed by the center of charge orbit, A_Φ , is an adiabatic invariant.

The adiabatic invariant is broken when the perturbation is applied rapidly compared to the diocotron period. The change in the adiabatic invariant, ΔA_Φ , depends on three factors: the perturbation rise time T_r , the perturbation strength V_p , and the phase θ , where θ is the angle between the position of the electron column and the angular sector at the moment the perturbation is first applied. The perturbation is linearly ramped for a time T_r . The following results have been obtained using the circular plasma model.

In Fig. 4, we show the phase dependence of ΔA_Φ by varying θ while keeping T_r and V_p constant. T_d is the diocotron period of the unperturbed system. Note that ΔA_Φ can be positive, negative, or zero, depending on the

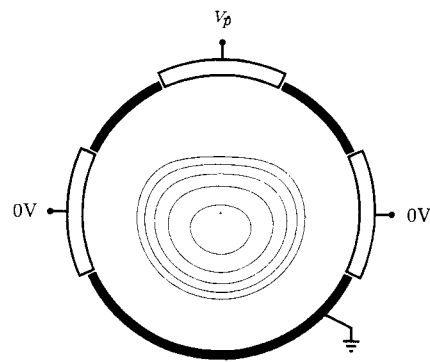


FIG. 3. A set of center of charge orbits determined by the line charge model (or the circular plasma model) for $V_p/enA_p = 1.15$.

phase at which the perturbation is turned on. The existence of both signs of ΔA_Φ is readily explained in the limit in which the perturbation is applied instantly. When there is no perturbation, the allowed orbits are a set of nested circles. The perturbation distorts these orbits into a set of noncircular closed loops. The instantaneously applied perturbation kicks the plasma column onto the perturbed orbit which crosses the unperturbed orbit at the column's position. Depending on θ this new orbit can have either greater or lesser area.

In Fig. 5, we show the maximum changes in A_Φ as a function of T_r . For each value of T_r , a scan over θ gives both the largest positive and negative values of ΔA_Φ . The oscillations seen in Fig. 5 have a period equal to the orbital period. Other examples of adiabatic breaking¹⁵ exhibit similar behavior.

The experimental results shown in Fig. 5 are in good

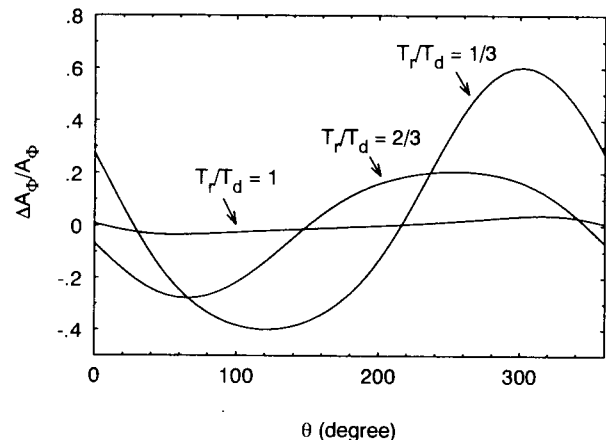


FIG. 4. ΔA_Φ vs θ , for $V_p/enA_p = 1.15$ and $A_{\Phi 0}/\pi R^2 = 0.14$ ($A_{\Phi 0}$ being the area enclosed by the unperturbed orbit).

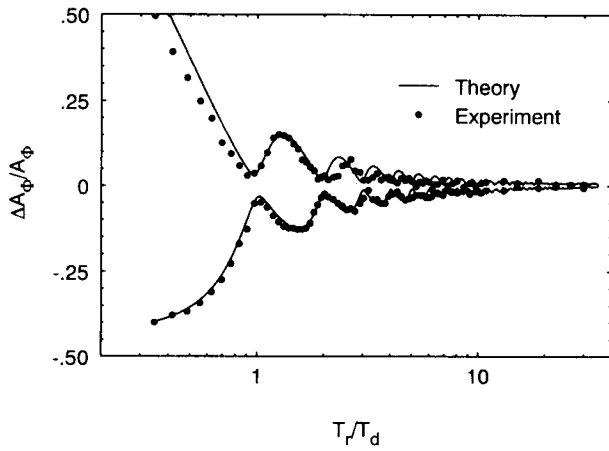


FIG. 5. Maximum and minimum ΔA_ϕ vs T_r/T_d for $V_p/enA_p = 1.15$ and $A_{\phi 0}/\pi R^2 = 0.14$. Corresponding experimental results⁷ are also plotted.

agreement with the results of the theoretical plasma model. The finite lengths of the experimental apparatus and the plasma require some modifications to the theory. In addition, the fields from the end cylinders (negatively biased coaxial cylinders which assure axial confinement of the plasma) which intrude into the plasma region play a more important role in bulk plasma dynamics than in static equilibria because these end fields are comparable to the image field of the plasma. These end fields speed up the diocotron motion, and hence reduce the influence of the applied perturbation on the orbit. A correction factor is obtained empirically by comparing the shape of the experimental orbit obtained with a known adiabatically applied sector bias to a theoretical orbit [found by solving Eqs. (21) and (22)]. The ratio of the experimental and theoretical biases which produce the same orbital shape is the desired correction factor. The time scale of the perturbation has been scaled by the ratio of the experimental and theoretical diocotron periods. The small discrepancy between the theoretical and

experimental results shown in Fig. 5 (for small T_r/T_d) is present even when the full elliptical plasma model is used; in fact the results of the elliptical plasma model and the circular plasma model are, for these parameters, nearly indistinguishable. Hence, this discrepancy is not attributed to the restrictions on the plasma shape. It may indicate that the full three-dimensional effects cannot be accounted for by our two empirical factors.

IV. LARGE AMPLITUDE $\ell=1$ AND $\ell=2$ DIOCOTRON MODES IN SYMMETRIC TRAPS

The elliptical plasma model developed in Sec. IV is also useful in studying coherent structures in symmetric traps, especially when the shape of the structures resembles an ellipse. The model is used to study the frequency and shape of the large amplitude $\ell=1$ and $\ell=2$ diocotron modes. Since there is no applied perturbation, $\phi_a = 0$. In order to improve the accuracy of the calculations, terms of order up to A_p^4 are now kept in the expansion in H_λ . The Hamiltonian consists of

$$H_s = -\frac{(enA_p)^2}{2} \ln\left(\frac{(1+\lambda)^2}{4\lambda}\right), \quad (24)$$

$$H_c = (enA_p)^2 \ln\left(1 - \frac{r_c^2}{R^2}\right), \quad (25)$$

$$H_\lambda = \frac{e^2 n^2 A_p^3 (1-\lambda^2)}{4\pi} \frac{r_c^2}{(R^2 - r_c^2)^2} \left\{ \cos 2(\theta_c - \varphi) - \frac{A_p}{8\pi} \left(\frac{1-\lambda^2}{\lambda}\right) \frac{1}{(R^2 - r_c^2)^2} \left[R^2 \left(\frac{R^2}{r_c^2} + 2\right) + 2r_c^2 \cos 4(\theta_c - \varphi) \right] \right\}. \quad (26)$$

Equations of motion are

$$\dot{r}_c = -\frac{cenA_p^2 r_c}{2\pi B (R^2 - r_c^2)^2} \left(\frac{1-\lambda^2}{\lambda}\right) \left[\sin 2(\theta_c - \varphi) - \frac{A_p r_c^2}{2\pi (R^2 - r_c^2)^2} \left(\frac{1-\lambda^2}{\lambda}\right) \sin 4(\theta_c - \varphi) \right], \quad (27)$$

$$\dot{\theta}_c = \frac{2cenA_p}{B (R^2 - r_c^2)} \left[1 - \frac{A_p (R^2 + r_c^2)}{4\pi (R^2 - r_c^2)^2} \left(\frac{1-\lambda^2}{\lambda}\right) \cos 2(\theta_c - \varphi) + \frac{A_p^2 (R^2 + r_c^2)}{16\pi^2 (R^2 - r_c^2)^4} \left(\frac{(1-\lambda^2)^2}{\lambda^2}\right) [3R^2 + 2r_c^2 \cos 4(\theta_c - \varphi)] \right], \quad (28)$$

$$\dot{\lambda} = -\frac{2cenA_p r_c^2}{B (R^2 - r_c^2)^2} \left(2\lambda \sin 2(\theta_c - \varphi) - \frac{A_p r_c^2 (1-\lambda^2)}{\pi (R^2 - r_c^2)^2} \sin 4(\theta_c - \varphi) \right), \quad (29)$$

$$\dot{\varphi} = \frac{2cen\pi}{B} \left[\frac{2\lambda}{(1+\lambda)^2} - \frac{A_p r_c^2}{\pi (R^2 - r_c^2)^2} \left(\frac{1+\lambda^2}{1-\lambda^2}\right) \cos 2(\theta_c - \varphi) + \frac{A_p^2}{4\pi^2} \left(\frac{1+\lambda^2}{\lambda}\right) \left(\frac{R^2 (R^2 + 2r_c^2) + 2r_c^4 \cos 4(\theta_c - \varphi)}{(R^2 - r_c^2)^4} \right) \right]. \quad (30)$$

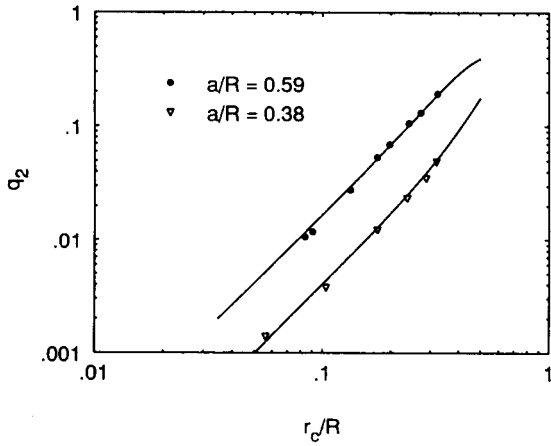


FIG. 6. Quadrupole moment, q_2 , vs r_c/R . Corresponding experimental results^{17,18} are also plotted.

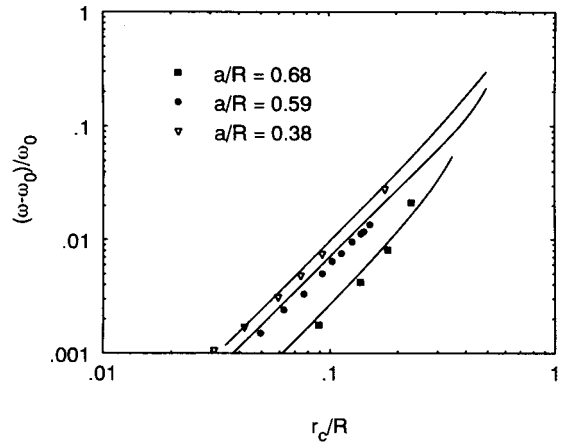


FIG. 7. Frequency shift vs r_c/R . Corresponding experimental results^{17,18} are also plotted.

In the experiments,¹⁶⁻¹⁸ the $\ell=1$ mode is observed as a dynamical structure which rotates around the center of the confining cylinder while its shape remains unchanged. The shape of the plasma closely resemble an ellipse with its major axis perpendicular to the radial vector. Since the plasma is stationary in a rotating frame with rotation frequency, ω , we look for the solution of the equations: $\dot{r}_c = 0$, $\dot{\lambda} = 0$, and $\dot{\theta}_c = \dot{\varphi} = \omega$. An elliptical plasma having its major axis perpendicular to the radial vector, i.e., $\varphi - \theta_c = \pi/2$, satisfies the requirements that $\dot{r}_c = 0$ and $\dot{\lambda} = 0$, according to Eqs. (27) and (29). Equations (28) and (30) reduce to

$$\dot{\theta}_c = \omega = \frac{2cenA_p}{B(R^2 - r_c^2)} \left[1 + \frac{A_p(R^2 + r_c^2)}{4\pi(R^2 - r_c^2)^2} \left(\frac{1 - \lambda^2}{\lambda} \right) + \frac{A_p^2(R^2 + r_c^2)(3R^2 + 2r_c^2)}{16\pi^2(R^2 - r_c^2)^4} \left(\frac{1 - \lambda^2}{\lambda^2} \right)^2 \right], \quad (31)$$

and

$$\dot{\varphi} = \omega = \frac{2cen\pi}{B} \left[\frac{2\lambda}{(1 + \lambda)^2} + \frac{A_p r_c^2}{\pi(R^2 - r_c^2)^2} \left(\frac{1 + \lambda^2}{1 - \lambda^2} \right) + \frac{A_p^2(R^4 + 2R^2 r_c^2 + 2r_c^4)}{4\pi^2(R^2 - r_c^2)^4} \left(\frac{1 + \lambda^2}{\lambda} \right) \right]. \quad (32)$$

Equating $\dot{\theta}_c$ and $\dot{\varphi}$ gives the aspect ratio of the plasma, λ , in terms of the displacement of its center, r_c , and the area of the plasma, A_p . Substituting λ back into the $\dot{\theta}_c$ equation or the $\dot{\varphi}$ equation yields the mode frequency, ω . Equation $\dot{\theta}_c = \dot{\varphi}$ can be solved numerically by a simple root finding routine. In Figs. 6 and 7, we compared our calculated results (lines) with experimental data (points) obtained by Fine, Driscoll, and Malmberg.^{17,18} In Fig. 6, $a \equiv \sqrt{A_p/\pi}$. The plasma elongation is characterized by its quadrupole moment, q_2 , which is defined as $q_2 \equiv (p_{xx} - p_{yy})/(p_{xx} + p_{yy})$, where $p_{xx} \equiv \int x^2 n(x,y) dx dy$, with a similar definition for p_{yy} . Here, the (x,y) coordinate system has its ori-

gin at the center of charge of the plasma and x lies along its long axis. For our constant density elliptical plasma, $q_2 = (\lambda^2 - 1)/(\lambda^2 + 1)$. In Fig. 7, $\omega_0 = (2cenA_p)/(BR^2)$ is the linear $\ell=1$ diocotron mode frequency.⁹ The agreements for both the shape and frequency are good.

In the case where the deviation of the shape from a circle is small, i.e., $\Delta\lambda \ll 1$, where $\Delta\lambda \equiv \lambda - 1$, due to a small displacement from the center, i.e., $r_c \ll R$, the equation $\dot{\theta}_c = \dot{\varphi}$ can be solved by linearization. Terms are kept up to order r_c^2 . In this limit, $q_2 = \Delta\lambda$. Linearizing the equation $\dot{\theta}_c = \dot{\varphi}$ gives

$$\Delta\lambda = \frac{2(a/R)^2(r_c/R)^2}{[1 - (a/R)^2]^2} \quad (33)$$

and

$$\frac{\omega - \omega_0}{\omega_0} = \frac{[1 - 2(a/R)^2](r_c/R)^2}{[1 - (a/R)^2]^2}. \quad (34)$$

These expressions are the same as those obtained recently by Fine.¹⁹ Other investigators have also studied this mode numerically.^{20,21}

We can also use the elliptical plasma model to calculate the frequency of a large amplitude $\ell=2$ diocotron mode because its shape is closely approximated by an ellipse.¹⁶ For this mode, the center of the plasma is not displaced from the axis of the confining cylinder, i.e., $r_c = 0$. According to Eqs. (27) and (29), $r_c = 0$ implies that $\dot{r}_c = 0$ and $\dot{\lambda} = 0$. In other words, an elliptical plasma with its center located on the axis of the confining cylinder will, in our model, remain on axis, without any change in the shape. θ_c is undefined since $r_c = 0$, and $\dot{\varphi}$ is the rotation frequency of the structure. Substituting $r_c = 0$ into Eq. (30) yields the rotation frequency as a function of the area and the ellipticity of the plasma,

$$\dot{\varphi} = \frac{2cen\pi}{B} \left[\frac{2\lambda}{(1 + \lambda)^2} + \frac{A_p^2}{4\pi^2 R^4} \left(\frac{1 + \lambda^2}{\lambda} \right) \right]. \quad (35)$$

The frequency from a standard linear theory⁹ can be recovered by putting $\lambda=1$ into the above expression.

V. SUMMARY

In this paper we have presented an analytic model which predicts the approximate shape of a non-neutral plasma confined in an asymmetric Penning trap. When the asymmetries are small, we have proved that these plasmas are stable to $\mathbf{E} \times \mathbf{B}$ drift perturbations by using an extremal energy principle analogous to that used by O'Neil and Smith.⁸ Since the angular momentum of these plasmas need not be conserved, the angular momentum conservation principle³ previously employed to prove confinement is not applicable. Hence, further studies are necessary to explain their lifetimes of tens of seconds.⁴ We have also explored the bulk dynamics of the analog of the $\ell=1$ diocotron mode using a Hamiltonian model. When the plasma is small, the elliptical simplification of this model shows that the evolution of the plasma shape and orientation has little effect on the center of charge orbit, thereby explaining the observed adiabatic invariant.⁷ The elliptical plasma model also successfully predicts the measured frequency and shape of the $\ell=1$ diocotron mode in symmetric traps.¹⁶⁻¹⁸ The frequency of the $\ell=2$ diocotron mode is also calculated. The model should also be useful in describing the breathing motion and oscillation of a nearly elliptical plasma when its initial shape or orientation deviates from the rotating $\ell=1$ diocotron mode equilibrium.

- ¹J. H. Malmberg, C. F. Driscoll, B. Beck, D. L. Eggleston, J. Fajans, K. Fine, X. P. Huang, and A. W. Hyatt, in *Nonneutral Plasma Physics*, AIP Conf. Proc. 175, edited by C. W. Roberson and C. F. Driscoll (American Institute of Physics, New York, 1988), p. 28.
- ²T. M. O'Neil, in Ref. 1, p. 1.
- ³T. M. O'Neil, *Phys. Fluids* **23**, 2216 (1980).
- ⁴J. Notte, A. J. Peurrung, J. Fajans, R. Chu, and J. S. Wurtele, *Phys. Rev. Lett.* **69**, 3056 (1992).
- ⁵R. H. Levy, *Phys. Fluids* **11**, 920 (1968).
- ⁶R. J. Briggs, J. D. Daugherty, and R. H. Levy, *Phys. Fluids* **13**, 421 (1970).
- ⁷J. Notte, J. Fajans, R. Chu, and J. S. Wurtele, "Experimental Breaking of an Adiabatic Invariant," submitted to *Phys. Rev. Lett.*
- ⁸T. M. O'Neil and R. A. Smith, *Phys. Fluids B* **4**, 2720 (1992).
- ⁹R. C. Davidson, *Physics of Nonneutral Plasmas* (Addison-Wesley, Reading, MA, 1990).
- ¹⁰M. V. Melander, N. J. Zabusky, and A. S. Styczek, *J. Fluid Mech.* **167**, 95 (1986).
- ¹¹B. Legras and D. G. Dritschel, *Phys. Fluids A* **3**, 845 (1991).
- ¹²D. G. Dritschel and B. Legras, *Phys. Fluids A* **3**, 855 (1991).
- ¹³T. B. Mitchell, C. F. Driscoll, and K. S. Fine, *Bull. Am. Phys. Soc.* **37**, 1415 (1992).
- ¹⁴L. D. Landau and E. M. Lifshitz, *Mechanics* (Pergamon, Elmsford, NY, 1976).
- ¹⁵J. E. Borovsky and P. J. Hansen, *Phys. Rev. A* **43**, 5605 (1991).
- ¹⁶C. F. Driscoll and K. S. Fine, *Phys. Fluids B* **2**, 1359 (1990).
- ¹⁷K. S. Fine, C. F. Driscoll, and J. H. Malmberg, *Phys. Rev. Lett.* **63**, 2232 (1989).
- ¹⁸K. S. Fine, Ph.D. dissertation, University of California, San Diego, 1988.
- ¹⁹K. S. Fine, *Phys. Fluids B* **4**, 3981 (1992).
- ²⁰S. M. Lund, J. J. Ramos, and R. C. Davidson, *Phys. Fluids B* **5**, 19 (1993).
- ²¹G. W. Mason and R. L. Spencer, *Bull. Am. Phys. Soc.* **37**, 1417 (1992).